

Evolution of nuclear structure through isomerism in ^{216}Fr

Madhu,¹ Khamosh Yadav,¹ A. Y. Deo^{1,*}, Pragati¹, P. C. Srivastava¹, S. K. Tandel,² S. G. Wahid², S. Kumar³, S. Muralithar,⁴ R. P. Singh,⁴ Indu Bala,⁴ S. S. Bhattacharjee^{4,†}, Ritika Garg,⁴ S. Chakraborty⁵, S. Rai,⁶ and A. K. Jain^{1,7}

¹*Department of Physics, Indian Institute of Technology Roorkee, Roorkee 247667, India*

²*School of Physical Sciences, UM-DAE Centre for Excellence in Basic Sciences, University of Mumbai, Mumbai 400098, India*

³*Department of Physics and Astrophysics, University of Delhi, New Delhi 110007, India*

⁴*Inter University Accelerator Centre, Aruna Asaf Ali Marg, New Delhi 110067, India*

⁵*Variable Energy Cyclotron Centre, Kolkata 700064, India*

⁶*State Forensic Science Laboratory, 37/1/2 Belgachia Road, Kolkata 700037, India*

⁷*Amity Institute of Nuclear Science and Technology, Amity University UP, Noida 201303, India*



(Received 26 November 2021; accepted 23 February 2022; published 4 March 2022)

Three new isomers have been identified in the transitional odd-odd ^{216}Fr nucleus. The properties of the (11^+) isomer with $T_{1/2} = 9.6(14)$ ns are compared with those of the similar isomeric states in neighboring doubly-odd nuclei. The experimental results are compared with predictions of shell-model calculations and a fair agreement is observed between the experimental and calculated excitation energies of the (11^+) isomeric state and the states to which it decays. The deviation between the measured and calculated reduced transition probabilities suggests contribution from effects other than the single-particle degrees of freedom in these states. Evidence of two high-spin [$J^\pi > (18^+)$] isomers above 2.2 MeV excitation energy with $T_{1/2} = 7.8(14)$ and 89(9) ns is also presented. These isomers at high excitation energies reflect a pronounced change in the structure above the previously established level scheme, where moderate quadrupole collectivity and octupole correlations were evident.

DOI: [10.1103/PhysRevC.105.034308](https://doi.org/10.1103/PhysRevC.105.034308)

I. INTRODUCTION

Excited metastable states which face an inhibition in their decay to low-lying states are termed isomers [1,2]. Although there is no stringent rule on the minimum half-life for a state to be classified as an isomer, excited states with half-life > 1 ns are generally considered isomers. The hindrance in the decay of a state can be attributed to a significant difference in the structure of the isomeric state and the states to which it decays, resulting in a reduced overlap between initial and final state wave functions. In most of the cases, a low energy and high multipolarity of the connecting γ -ray transition leads to a longer half-life of the initial state. Depending on the hindrance mechanism, isomers can be categorized into different types such as spin isomers, shape isomers, K isomers, etc. [1,2]. The understanding of the formation and the decay of isomers reveals important aspects of nuclear structure and tests the predictions of various nuclear models. In addition to providing insights into nuclear structure, isomers have interesting applications in the fields of medicine and astrophysics [3].

The region around the doubly magic nucleus ^{208}Pb is known for a wealth of isomerism [2]. The availability of high- j proton and neutron orbitals governs the nuclear structure

and isomer formation in this region. Low-lying states in ^{212}Rn and ^{214}Ra ($N = 126$ isotones) are members of the multiplets based on the $\pi h_{9/2}^4$ and $\pi h_{9/2}^6$ configurations, respectively [4,5]. In both these nuclei, states with $J^\pi = 4^+$, 6^+ , and 8^+ have been identified as seniority isomers. The small $E2$ transition strengths between states with the same seniority near the middle of the valence shell along with the decreasing energy spacing in a multiplet with increasing spin give rise to longer half-lives of these states. Also, a large number of isomers deexciting via enhanced $E3$ transitions have been identified in near-spherical At-Rn-Fr nuclei [6–9]. Their properties such as excitation energies, $E3$ decay path, transition strengths, etc. are understood in terms of the multiparticle octupole coupling model [9–11].

As one moves away from the near-spherical region with the addition of valence nucleons, collective modes of excitation become important. The nuclei in the Ra-Th ($Z \approx 88$ and $N \approx 134$) region exhibit features of static octupole deformation [12–15] and are known to possess a fewer number of isomers. Also, it was recently suggested that the properties of high- K isomeric states in heavy even-even actinides may play a pivotal role in determining the degree of octupole collectivity in these nuclei [16].

The francium ($Z = 87$) isotopes with $126 \leq N \leq 129$ lie at the lower mass boundary beyond which the octupole correlations emerge in the trans-lead region [15]. The structure of ^{215}Fr ($N = 128$) is mainly dominated by single-particle excitations [17], while in ^{217}Fr ($N = 130$), the octupole

*Corresponding author: ajay.deo@ph.iitr.ac.in

†Present address: Institute of Experimental and Applied Physics, Czech Technical University in Prague, Husova 240/5, 110 00 Prague 1, Czech Republic.

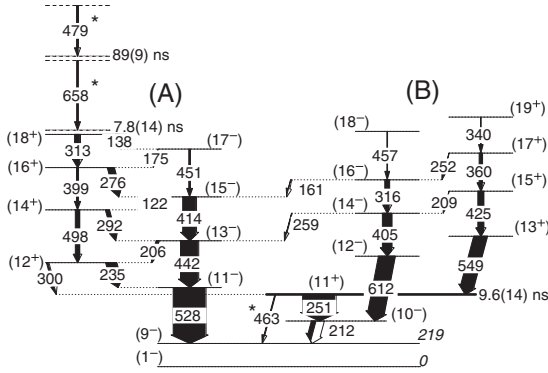


FIG. 1. Partial level scheme of ^{216}Fr established in the earlier work [19]. The newly identified transitions are marked with an asterisk.

correlations are manifested in the form of alternating parity bands connected by enhanced $E1$ transitions [18]. A recent study by Pragati *et al.* has confirmed that ^{216}Fr , which has $Z = 87$ and $N = 129$, is the lightest nucleus to exhibit octupole correlations in this region [19]. Thus, the search for isomers in ^{216}Fr and their interpretation could provide a better understanding of the evolution from the single-particle to collective excitations.

In the earlier studies of ^{216}Fr , two low-lying isomers with $J^\pi = (3^-)$ and (9^-) were reported at 133 and 219 keV excitation energies, respectively [20–22]. The isomeric 8^- or 9^- states observed in most of the odd-odd nuclei in the trans-lead region arise from the $\pi h_{9/2} \otimes \nu g_{9/2}$ configuration and provide information on the residual interaction between the unpaired $h_{9/2}$ proton and $g_{9/2}$ neutron. In the present work, we report the observation of three new isomers in ^{216}Fr .

II. EXPERIMENTAL DETAILS AND RESULTS

High-spin states in ^{216}Fr were populated using the $^{208}\text{Pb}(^{11}\text{B}, 3n)^{216}\text{Fr}$ reaction in an experiment performed at the Inter University Accelerator Centre (IUAC), New Delhi. A self-supporting ^{208}Pb target with a thickness of ≈ 6 mg/cm 2 and 99% enrichment was bombarded with a ^{11}B beam in the 54–62 MeV energy range. The γ rays emitted in the deexcitation process of residual nuclei were detected using the Indian National Gamma Array (INGA), which consisted of 14 Compton-suppressed clover detectors at the time of the experiment. The detectors were placed at 90° , 123° , and 148° with respect to the beam direction.

Figure 1 illustrates a part of the level scheme of ^{216}Fr which was reported recently in Ref. [19]. The coincidence relationships between the γ rays were established using a symmetric $\gamma - \gamma$ matrix and $\gamma - \gamma - \gamma$ cube. The multiplicities of the observed γ rays were determined by measuring ratios of directional correlations of oriented states (R_{DCO}) [23] and polarization asymmetry (Δ_{asym}) [24]. The detailed information concerning the experimental setup and the data analysis procedure is given here [19]. The present work mainly focuses on the search of isomeric states in ^{216}Fr . The half-lives of the isomers were extracted using centroid-shift and decay-curve analyses. The choice of the method is dictated by the lifetime

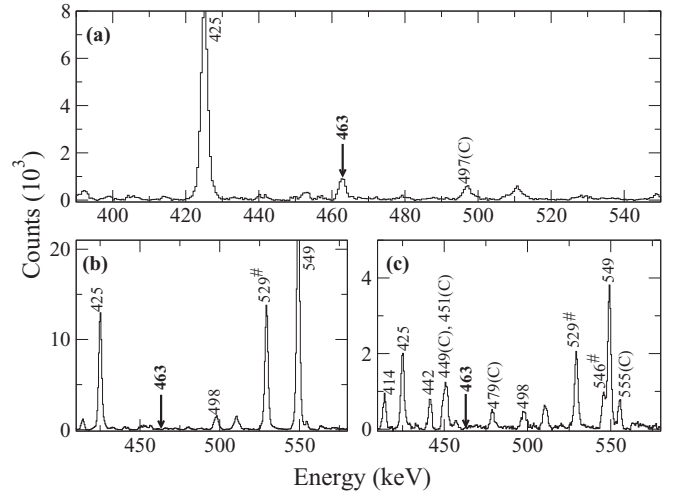


FIG. 2. Coincidence γ -ray spectra showing transitions in the gate of the (a) 549-, (b) 251-, and (c) 212-keV transitions. The contaminant peaks, mainly from ^{215}Fr , are marked with “C”. The transitions indicated by “#” belong to ^{216}Fr and their placement is discussed elsewhere [27]. The presence/absence of the 463 keV γ ray is also indicated.

of the state and time resolution of the detection setup. Lifetimes greater than the full width at half maximum (FWHM) of the corresponding prompt distribution can be extracted using decay-curve analysis. On the other hand, centroid-shift analysis is used to determine lifetimes which are smaller compared to the FWHM of the prompt distribution [25]. It may be noted that the FWHM for the present detection setup was around 50 ns. For this purpose, the calibrated data were written into a ROOT [26] tree format. The ROOT tree was used to construct a three-dimensional histogram with *early* γ rays along the X axis, *delayed* γ rays along the Y axis and their time difference (ΔT) along the Z axis.

A. (11^+) isomer at $E_x = 682$ keV

The recent study by Pragati *et al.* [19] established a simplex partner band (B) of the previously known structure (A) in ^{216}Fr , as shown in Fig. 1. Below, we will discuss the placement of the transitions, relevant for the present discussion on isomers, which are being reported in this paper for the first time. Figure 2 illustrates the coincident γ -ray transitions in the gate of the (a) 549-, (b) 251-, and (c) 212-keV transitions. A comparison of the spectra (see Fig. 2) demonstrates the placement of the 463-keV transition, as shown in Fig. 1. Furthermore, the R_{DCO} value for the 463-keV γ ray is found to be 1.10(9) in the gate of a $\Delta J = 2$ transition, which indicates the quadrupole nature of the γ ray.

Figure 3 shows *early* coincident transitions within 50–200 ns time range in the gate of the 251-keV γ ray. The presence of the intense 549-keV γ ray which directly feeds the (11^+) level and the other higher-lying transitions in the spectrum indicate the metastable nature of the (11^+) state. The half-life of this state is determined using the centroid-shift technique. In Fig. 4, the time-difference curve between γ -ray transitions feeding and de-exciting the (11^+) level, after

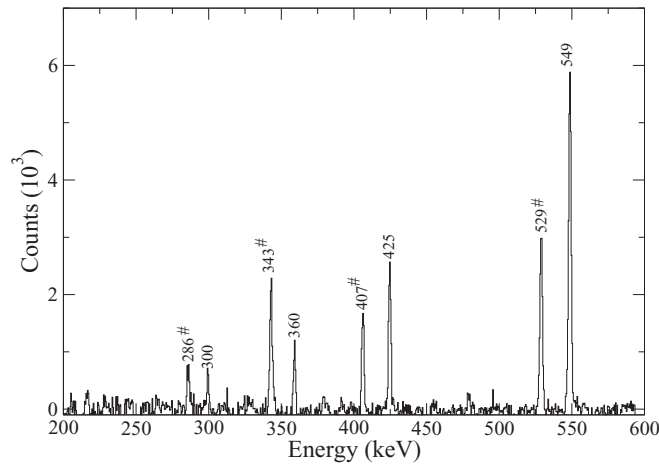


FIG. 3. γ -ray spectra illustrating *early* transitions in the gate of the 251 keV γ ray. The transitions indicated by “#” belong to ^{216}Fr and their placement is discussed elsewhere [27].

taking proper background subtraction into account, is shown in blue color. Considering the energy dependence of the time response of the detectors, another time-difference histogram is generated for transitions with similar energies (to that of transitions feeding and deexciting the isomeric state) which are in prompt coincidence with each other. The difference between the centroids of the two distributions gives the mean life of the state. From the above analysis, $T_{1/2} = 9.6(14)$ ns is inferred for the (11^+) state. The total error quoted in the half-life is obtained by adding the systematic and statistical errors in quadrature. The systematic error for centroid-shift analysis includes contributions from the discrete binning along the time axis and the uncertainty arising due to shift in the centroid

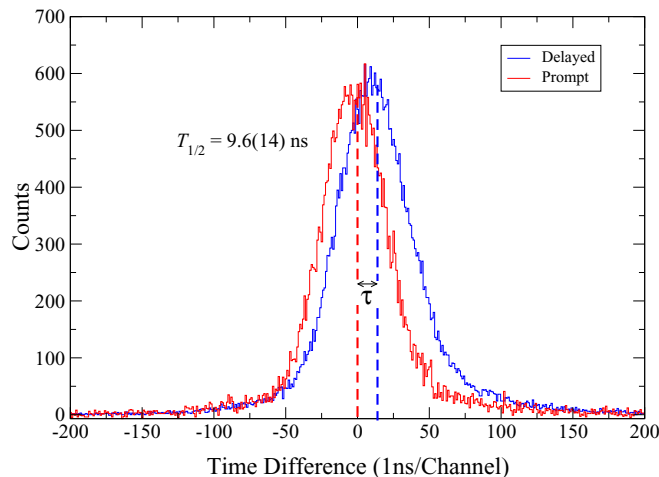


FIG. 4. Time-difference spectra illustrating the centroid-shift technique used for determining the half-life of the (11^+) state. The blue histogram represents the time difference between the 549- and 251-keV γ rays, feeding and depopulating the (11^+) state, respectively. The time difference between two prompt transitions of similar energies is shown in red color. The difference in the centroids of the distributions gives the mean life of the state.

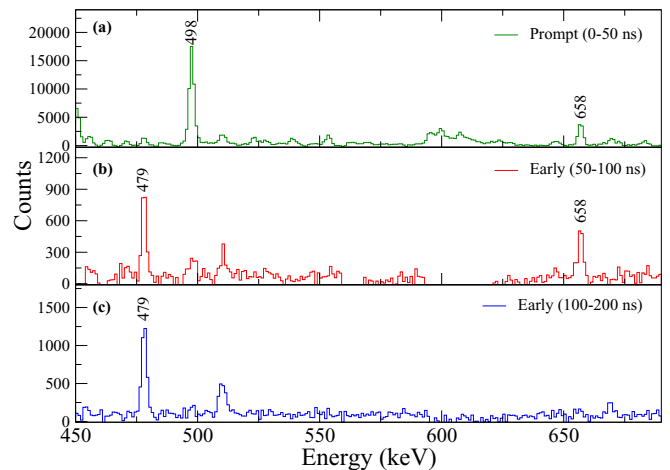


FIG. 5. γ -ray spectra within (a) prompt, (b) *early* (50–100 ns), and (c) *early* (100–200 ns) time windows in the gate of the 528 keV transition.

of the prompt distribution of two similar energy transitions. Thus, the total systematic uncertainty for the centroid-shift analysis is found to be 1.34 ns. Also, the statistical uncertainties in the centroids of the prompt and delayed distributions are taken into account. The contribution of the total statistical error in the half-life of the (11^+) state is found to be 0.17 ns.

B. Evidence of isomers above the (18^+) state

Figure 5 illustrates coincidence spectra in the gate of the 528-keV γ ray for three different time windows as indicated. The observation of 479- and 658-keV transitions in the 50–100 ns *early* spectrum [Fig. 5(b)] indicates the presence of one or more isomeric states. However, as shown in Fig. 5(c), only the 479-keV γ ray is observed in the 100–200 ns time window. The absence of the 658 keV transition suggests that two different metastable states are populated by the 479- and 658-keV γ rays and the state populated by the 479-keV transition is expected to have a longer half-life than the one populated by the 658-keV γ ray.

Furthermore, the presence of the 479-keV transition in the delayed gate of the 658-keV γ ray, as shown in Fig. 6, establishes the coincidence relationship between these transitions. This, in turn, implies that the isomeric state populated by the 479-keV γ ray lies at higher excitation energy than that populated by the 658-keV γ ray. Thus, two high-spin isomers are identified above the (18^+) level. The possible reasons for the isomeric nature of these states are discussed below. One possibility could be the presence of low energy and/or highly converted γ -ray transitions in the decay path of the isomers, which is depicted in Fig. 1. However, such transitions could not be detected with the present experimental setup. Another possibility could be that the state which is being populated by the 479-keV transition deexcites directly via hindered $M2$ or enhanced $E3$ 658-keV transition. Due to poor statistics, the multipolarity of the 658-keV transition could not be determined. Therefore, the decay path and hence the excitation energies and spin-parities of these isomers at

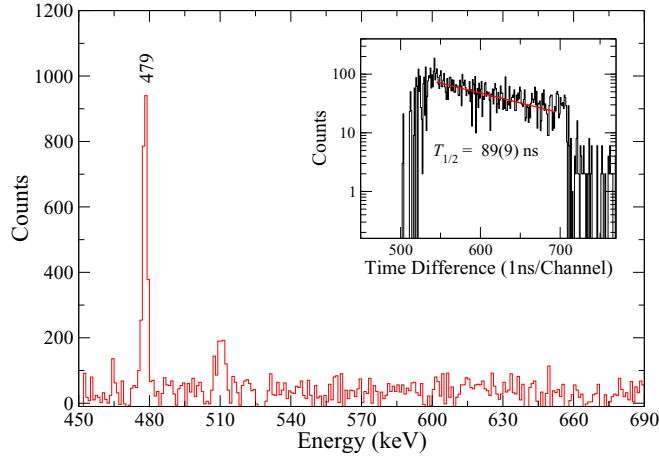


FIG. 6. γ -ray spectra within the *early* (100–200 ns) time window in the gate of the 658 keV transition. The inset shows the decay curve obtained using the 479 keV (start) and the 658 keV (stop) γ rays.

high-excitation energies could not be determined. Preliminary results concerning the evidence of these high-spin isomers were reported earlier [28].

The centroid-shift analysis was performed to extract the half-life of the isomer populated by the 658-keV transition. The time difference spectrum of the 658- and 313-keV transitions is compared with that generated using the prompt transitions of similar energies (see Fig. 7). This yields $T_{1/2} = 7.8(14)$ ns for the state populated by the 658-keV transition. The error quoted here is the combination of total systematic uncertainty (1.34 ns) and the statistical error (0.52 ns) added in quadrature. The inset of Fig. 6 shows the decay curve obtained using the 479-keV transition (start) and the 658-keV transition (stop). The half-life for the isomer populated by the 479-keV transitions is found to be 89(9) ns.

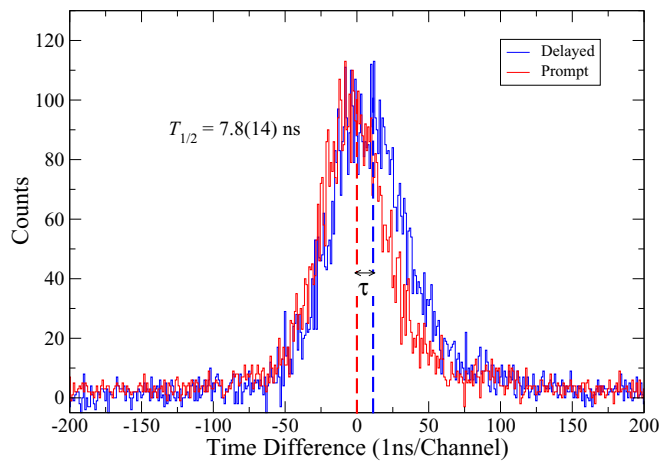


FIG. 7. Half-life of the isomeric state populated by the 658 keV γ ray is determined using the centroid-shift technique. The time difference spectrum for the 658- and 313 keV γ rays is compared with that obtained using two prompt transitions with similar energies. The difference in the centroids of the distributions yields the mean life of the state.

III. DISCUSSION

The region just above the $Z = 82$ and the $N = 126$ shell closure is rich in nuclear isomerism [2,29]. A recent compilation on isomers with $T_{1/2} \geq 10$ ns tabulates the excitation energies, half-lives, and decay modes of the metastable states [30]. The highest spin isomer known in the nuclear chart has been reported in ^{212}Rn with $J^\pi = (38)^+$ at an excitation energy of 12.5 MeV [4]. The triple neutron core-excitations coupled to mutually aligned proton orbitals contribute to angular momentum in the $J \geq 20\hbar$ regime in this nucleus. The properties of the (25^-) isomeric state [$T_{1/2} = 152(5)\mu\text{s}$] in ^{212}At are understood in terms of the blocking of octupole correlations due to occupation of the single-particle $\nu i_{11/2}$ orbital [31]. Also, several spin isomers have been identified in ^{214}Fr and ^{215}Fr [6,17]. As mentioned earlier in Sec. I, two low-lying (3^-) and (9^-) isomers are known in ^{216}Fr . The (3^-) isomeric state at 133 keV excitation energy decays via both γ -ray and α -particle emission, whereas the (9^-) state at 219 keV decays mainly via α -particle emission. The electromagnetic decay of this state is hindered, as the excitation energies of the states corresponding to the $\pi h_{9/2} \otimes \nu g_{9/2}$ multiplet are expected to follow an inverted parabolic structure and the spacing between the levels of the multiplet decreases with increasing valence nucleons [20,32].

A. Low-lying (11^+) isomer

An (11^+) isomeric state has been reported in several odd-odd nuclei in this region. In ^{212}At and ^{218}Ac , this isomer decays by competing $M2$ and $E1$ transitions [8,33,34]. However, the (11^+) state in ^{214}Fr deexcites by a strong $M2$ and comparatively weak $E3$ γ ray [6]. In the earlier high-spin studies [19,35], no such isomer was reported in ^{216}Fr . As discussed earlier, we have established the isomeric character of the (11^+) state in ^{216}Fr in the present work.

Since ^{216}Fr is a transitional nucleus, both single-particle and collective behavior are expected to manifest in its level structure. The lowest-lying yrast (1^-) and (9^-) states are well accounted for by the spherical shell model and the states above the (11^+) isomer may be understood in terms of the reflection-asymmetric tidal wave approach [19,36]. Therefore, the nature of the isomeric state and the states to which it decays is important for understanding the evolution of structure in this transitional nucleus. Thus, the characteristics of the observed (11^+) isomer in ^{216}Fr are compared with those of a similar isomeric state in ^{212}At and ^{218}Ac . The (11^+) state in ^{216}Fr decays via the 251-keV $E1$ γ ray to the (10^-) level and the 463-keV $M2$ transition to the (9^-) state. Table I shows the transition energies, γ -ray branching ratios, reduced transition probabilities and single-particle transition rates for the decay paths of the (11^+) isomeric state in these doubly odd nuclei. The decay path of this isomer in ^{216}Fr is slightly different than that of the similar isomers in neighboring doubly odd nuclei in that the $M2$ branch is comparatively much weaker than the $E1$ branch in this nucleus, whereas the opposite is true in ^{212}At and ^{218}Ac . The ratio $\frac{\lambda(E1)}{\lambda(M2)}$ is of the order of 10^5 in ^{212}At and ^{218}Ac , while it is $\approx 10^6$ for ^{216}Fr . The enhancement can be attributed to the distribution of the energy difference [between

TABLE I. Comparison of the excitation energies (E_x) and the half-lives ($T_{1/2}$) of the (11^+) isomeric state in the doubly odd nuclei. γ -ray energies (E_γ), γ -ray branching ratios (γ_{BR}), reduced transition probabilities [$B(\sigma L)$] and single-particle transition rates [$\lambda(\sigma L)$] for the transitions depopulating the (11^+) state are also listed. The data for ^{212}At and ^{218}Ac are taken from Refs. [8] and [34], respectively.

Nucleus	E_x (keV)	$T_{1/2}$ (ns)	J_f^π	E_γ (keV)	Mult(σL)	γ_{BR} (%)	$B(\sigma L)$ ($e^2 fm^2$ or $\mu_N^2 fm^2$) ^a	$\lambda(\sigma L)$ (s^{-1})
^{212}At	885	18.7(7)	(10^-)	184	$E1$	33(3)	$1.1(5) \times 10^{-6}$	2.2×10^{13}
			(9^-)	662	$M2$	67(3)	12(1)	1.0×10^8
^{218}Ac	507 + Y	103(11)	(10^-)	91	$E1$	46(14)	$1.5(7) \times 10^{-6}$	2.7×10^{12}
			(9^-)	384	$M2$	54(9)	18(3)	6.6×10^6
^{216}Fr	682	9.6(14)	(10^-)	251	$E1$	98.4(7)	$2.6(4) \times 10^{-6}$	5.7×10^{13}
			(9^-)	463	$M2$	1.6(1)	3.8(6)	1.7×10^7

^aUnits correspond to the reduced transition strengths for the $E1$ and $M2$ transitions, respectively.

the (11^+) and (9^-) states] between $E1$ and $M2$ transitions (see Table I) which favors the stronger $E1$ branch in ^{216}Fr as opposed to the $M2$ in the other two nuclei.

The experimental $B(E1)$ and $B(M2)$ values were deduced for the 251- and 463-keV transitions, respectively, using the measured half-life [9.6(14) ns] of the (11^+) state, the branching ratios and the conversion coefficients. The states lying above the (11^+) isomer in ^{216}Fr form alternating parity sequences which are connected by $E1$ transitions. The enhanced $E1$ transitions are observed in nuclei with an intrinsic dipole moment such as nuclei with cluster structure or reflection asymmetry, in which case the $B(E1)$ values range from 10^{-2} to $10^{-3} e^2 fm^2$. The experimental $B(E1)$ value for the 251-keV γ ray is of the order of $10^{-6} e^2 fm^2$, which is 3–4 orders of magnitude smaller than what is expected for the collective transitions. This suggests that the 251-keV transition has a different origin than the $E1$ transitions observed in nuclei with an intrinsic dipole moment. The measured electric dipole reduced transition probability for the 251-keV γ ray indicates the single-particle nature of the states of interest. Thus, for a more quantitative understanding, large-scale shell-model calculations were employed for the states related to the decay path of the isomer.

The shell-model calculations were performed with the effective interaction derived from the CD-Bonn NN potential using the $V_{\text{low-}k}$ normalization approach [37] and the KSHELL code [38]. The valence space for protons consisted of $0h_{9/2}$, $1f_{7/2}$, $0i_{13/2}$, $1f_{5/2}$, $2p_{3/2}$, and $2p_{1/2}$ orbitals, while the neutron valence space included $1g_{9/2}$, $0i_{11/2}$, $0j_{15/2}$, $2d_{5/2}$, $3s_{1/2}$, $1g_{7/2}$, and $2d_{3/2}$ orbitals. The protons and neutrons were allowed to occupy any orbital, without any restrictions, in their corresponding valence space. The single-particle energies for protons and neutrons are taken from the experimental energies in ^{209}Bi and ^{209}Pb , respectively [39]. The predictions of the calculations are compared with the experimental results in Fig. 8 and the dominant configurations associated with the states of interest are mentioned. It is observed that the calculated excitation energies are in reasonable agreement with the experimental energies. The calculations suggest $\pi h_{9/2} \otimes \nu g_{9/2}$ configuration for the (9^-) state, which is consistent with the expected configuration for the yrast (9^-) state based on the systematics of the odd-odd nuclei in this region. Also, the dominant configurations obtained from the shell model for the

(10^-) and (11^+) states are in agreement with those suggested for the similar states in ^{212}At and ^{218}Ac .

Furthermore, the reduced transition probabilities for the (11^+) \rightarrow (9^-) and (11^+) \rightarrow (10^-) transitions were determined using the wave functions obtained from the shell-model calculations and the experimental transition strengths were compared with the calculated ones. The calculated $B(M2)$ of $111.5 \mu_N^2 fm^2$ is overpredicted compared to the measured value of $3.8(6) \mu_N^2 fm^2$ for the $M2$ transition. Also, the calculated $B(E1)$ value for the (11^+) \rightarrow (10^-) γ ray is found to be $< 10^{-10} e^2 fm^2$, which is several orders of magnitude smaller than the measured $B(E1)$ of $2.6(4) \times 10^{-6} e^2 fm^2$. In the calculations, the effective charges for protons and neutrons were taken as $e_\pi = 1.5e$ and $e_\nu = 0.5e$, respectively. Also, the orbital and spin g factors for protons and neutrons were assumed to be same as for the free nucleons.

It is known that the reduced matrix element of an electromagnetic operator depends on the multipole operator and the wave functions of the initial and final states [40]. Therefore, a deviation between the calculated and experimental values may arise if the wave functions of the states involve contributions

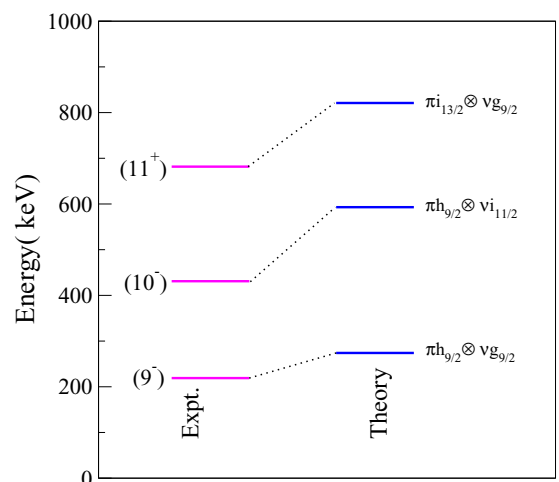


FIG. 8. Comparison of the low-lying experimental states relevant to the decay of the (11^+) isomer in ^{216}Fr with the shell-model predictions.

from the collective degrees of freedom which are not included in the shell-model approach and/or if the multipole operator does not include the effects of interactions between nucleons. The experimental $B(M2)$ value in ^{212}At was found to be in excellent agreement with the empirical $B(M2)$ calculated using the matrix element extracted from the $13/2^+ \rightarrow 9/2^-$ (1.609 MeV) transition in ^{209}Bi [33]. It is interesting to note that the $13/2^+$ state in ^{209}Bi is not a pure single-particle $\pi i_{13/2}$ state since it involves admixtures from the coupling of the $h_{9/2}$ proton to the 3^- octupole vibration in ^{208}Pb [41]. In addition, the core-polarization and mesonic effects were included in the empirical calculations. These effects can be accounted for in the shell-model calculations by using the effective orbital and spin g factors [42]. Although the effective g factors depend on the orbital and the nucleus, the standard values of $g_s^{eff} = 0.7g_s^{free}$ and $\delta g_l = 0.1$, for this region, were used in further calculations [42]. However, the $B(M2)$ value ($46\mu_N^2\text{fm}^2$) obtained using the effective magnetic operator is still 10 times more than the measured value. Further, g -factor measurements in future may provide more information on the possible admixtures, if any, in the wave function of the (11^+) isomer.

B. Isomers above the (18^+) state

It is well known that the nuclei in the $A \approx 220$ region present some of the best examples of reflection asymmetry in the nuclear chart. Calculations based on the cranked Wood-Saxon-Bogolyubov-Strutinsky approach were earlier employed to understand the evolution of shape with spin in Ra and Th nuclei (for $130 \leq N \leq 138$) [43]. It was predicted that the nuclei with small deformations at low and intermediate spins develop static octupole deformation at higher spins. In the case of heavier isotopes, with ground state quadrupole and octupole deformation, alternating parity bands which are a signature of octupole correlations are expected to terminate at high spins. The mean field calculations for ^{222}Th have predicted a shape transition at $\hbar\omega \approx 0.20$ MeV such that reflection symmetric bands become yrast at $J \geq 24\hbar$ [43]. A recent study of ^{223}Th presented experimental evidence of a band crossing at $\hbar\omega = 0.23$ MeV indicating a shape change from octupole to quadrupole shape [44]. Similar behavior has been observed in the $A \approx 150$ mass region where reflection symmetric structures coexist with alternating parity bands in ^{150}Sm [45].

However, the situation is more complex in ^{216}Fr wherein the level structures at low and intermediate energies are governed by single-particle and collective degrees of freedom, respectively. As reported in the previous section, we have identified two isomers at high-excitation energies in the present work. Figure 1 shows the partial level scheme of ^{216}Fr with the proposed high-spin isomeric states placed above the already observed level structure. If the alternating-parity sequences had persisted till higher spins in this nucleus, it would have been very unlikely to observe any isomers in that spin region. The presence of the observed high-spin isomers in ^{216}Fr indicates the possible shape change in the high-excitation energy regime. It may also be noted that

alternating parity sequences were predicted to terminate at 2.6 MeV excitation energy in ^{218}Ac [34].

Further, the available experimental information is not sufficient to unambiguously determine the spin-parity and the excitation energy of the proposed isomeric states. As discussed in Sec. II, the possible presence of low-energy and/or highly converted γ rays in the decay path could result in the metastable nature of the states populated by the 658- and 479-keV transitions. The half-life [7.8(14) ns] of the isomeric state populated by the 658-keV transition excludes the possibility of $M2$, $E3$, or higher multipolarity of the transition deexciting this state. In ^{217}Ra , which is an isotone of ^{216}Fr , a $33/2^+$ isomer with $T_{1/2} = 4.62(6)$ ns has been identified at 2.4 MeV excitation energy [46,47]. This isomer decays via an enhanced $E2$ transition of 92.5 keV and is populated by a 864-keV γ ray. Although the half-life for a low-energy (≤ 100 keV) $E2$ transition would be ≈ 100 ns, enhancement in $E2$ decays leads to much shorter lifetimes as compared to the expected values. Similar enhancement is also observed in ^{216}Fr where a low-lying (5^-) state, which deexcites via a 57.9 keV $E2$ γ ray, is not isomeric [22,48]. At intermediate excitation energies, alternating parity sequences connected by $E1$ transitions are observed in both ^{216}Fr and ^{217}Ra . The similarity in the level structures of these $N = 129$ isotones suggests an $E2$ multipolarity for the unobserved transition deexciting the isomeric state with $T_{1/2} = 7.8(14)$ ns in ^{216}Fr . This, in turn, suggests $J^\pi = (20^+)$ for the isomeric state under consideration. Assuming the same neutron configuration as for the $33/2^+$ isomeric state in ^{217}Ra , the (20^+) state in ^{216}Fr may be realized from $\pi(h_{9/2}^4 i_{13/2}) \otimes \nu(g_{9/2}^2 i_{11/2}^2)$ configuration. Also, the (20^+) state in ^{218}Ac is associated with a predominant $\pi(h_{9/2}^7)$ \otimes $\nu(g_{9/2}^2 j_{15/2})$ configuration. However, the shell-model calculations predict dominant contributions from $\pi(h_{9/2}^5)$ \otimes $\nu(g_{9/2} i_{11/2} j_{15/2})$ and $\pi(h_{9/2}^4 i_{13/2}) \otimes \nu(g_{9/2}^2 i_{11/2})$ configurations for the (20^+) state in ^{216}Fr . In ^{215}Fr , a $33/2^+$ isomeric state is observed at 2.2 MeV energy, and is interpreted as arising from $\pi(h_{9/2}^4 i_{13/2}) \otimes \nu(g_{9/2} i_{11/2})$ configuration [49]. The coupling of the extra $g_{9/2}$ neutron to this configuration leads to $\pi(h_{9/2}^4 i_{13/2}) \otimes \nu(g_{9/2}^2 i_{11/2})$ configuration for the (20^+) state in ^{216}Fr , which is in accordance with the configuration suggested by the shell-model calculations.

For the highest lying isomer, two decay paths are possible as discussed in Sec. II. The isomeric state either depopulates via a low-energy and/or highly converted γ ray followed by the 658-keV transition or it directly de-excites via hindered $M2$ or enhanced $E3$ 658-keV transition. In the first case, since the multipolarity of the 658-keV transition is unknown, it is not possible to propose spin-parity for the isomeric state under consideration. In the case of second possibility, the isomer may have $J^\pi = (22^-)$ or (23^-) . The shell-model calculations suggest an admixture of $\pi(h_{9/2}^4 i_{13/2}) \otimes \nu(g_{9/2} i_{11/2} j_{15/2})$ and $\pi(h_{9/2}^4 i_{13/2}) \otimes \nu(g_{9/2}^2 j_{15/2})$ configurations for the (22^-) state, whereas $\pi(h_{9/2}^4 i_{13/2}) \otimes \nu(g_{9/2} i_{11/2} j_{15/2})$ has been suggested as the dominant configuration for the (23^-) state. An (22^-) isomeric state, which decays via competing $M2$ and $E3$ branches, has also been reported in the doubly odd ^{212}At [8]. The second configuration [$\pi(h_{9/2}^4 i_{13/2}) \otimes \nu(g_{9/2}^2 j_{15/2})$]

proposed by the shell-model calculations for the (22^-) state in ^{216}Fr is consistent with the $\pi(h_{9/2}^2 i_{13/2}) \otimes \nu(j_{15/2})$ configuration assigned to the same state in ^{212}At . However, in the absence of sufficient experimental information it is not possible to firmly assign the spin-parities and excitation energies to these isomers in ^{216}Fr . In order to establish the decay path of these isomeric states with certainty and study the evolution of structure at high spin, spectroscopy experiments with a low-energy photon spectrometer (LEPS) and conversion-electron spectrometers with pulsed beam are desired.

IV. SUMMARY

An (11^+) isomer, which was known in several odd-odd nuclei in the trans-lead region, has been identified for the first time in ^{216}Fr . The half-life of the (11^+) state is found to be 9.6(14) ns using the centroid-shift technique. Large-scale shell-model calculations have been performed to understand the nature of the isomeric state and low-lying states. The experimental level energies are observed to agree well with calculated energies. The calculations have suggested $\pi i_{13/2} \otimes \nu g_{9/2}$ configuration for the isomeric state which is consistent with the configuration assigned to the (11^+) isomer in the neighboring doubly odd nuclei. However, the deviation between the measured and calculated transition strengths for the $(11^+) \rightarrow (9^-)$ and $(11^+) \rightarrow (10^-)$ transitions implies that effects which were not taken into account in the shell-model calculations play an important role in the states of interest. Two high-spin isomers have been identified in the present work and their half-lives have been reported. The presence of isomers above the (18^+) state suggests a pronounced change

in structure at high-excitation energy. Due to the experimental limitations, their decay path could not be identified and hence their spin-parities and excitation energies could not be unambiguously determined. In future, high-spin studies with LEPS detectors and conversion-electron spectrometer are required for establishing the decay path of these high-spin isomers. Finally, it may be noted that ^{216}Fr presents an interesting example wherein the simultaneous occurrence of isomers at low and high excitation energies is observed in a system which displays single-particle excitations and octupole correlations.

ACKNOWLEDGMENTS

The authors would like to thank P. Walker for his valuable comments and suggestions. The authors gratefully acknowledge the IUAC support staff for their assistance during the experiment. The authors would like to thank the INGA Collaboration for their help and support. Madhu would like to acknowledge the financial support from Department of Science and Technology (DST), India under the INSPIRE fellowship scheme (IF 180082). A.Y.D. acknowledges the financial support by Science and Engineering Research Board (SERB, DST), Grant No. CRG/2020/002169. K.Y. would like to acknowledge the support from the Ministry of Human Resource Development, India. P.C.S. acknowledges a research grant from the SERB (DST), India, CRG/2019/000556. S.K.T. thanks the University Grants Commission (UGC), India, for support under the Faculty Recharge Programme. A.K.J. acknowledges the financial support from SERB (DST), Grant No. CRG/2020/000770. The financial support by DST, India (Grant No. IR/S2/PF-03/2003-III) for the INGA project is acknowledged.

-
- [1] P. M. Walker and G. D. Dracoulis, *Nature (London)* **399**, 35 (1999).
- [2] A. K. Jain, B. Maheshwari, and A. Goel, *Nuclear Isomers: A Primer* (Springer Nature, Berlin, 2021).
- [3] P. M. Walker and J. J. Carroll, *Phys. Today* **58**(6), 39 (2005).
- [4] G. D. Dracoulis, G. J. Lane, A. P. Byrne, P. M. Davidson, T. Kibédi, P. H. Nieminen, H. Watanabe, A. N. Wilson, H. L. Liu, and F. R. Xu, *Phys. Rev. C* **80**, 054320 (2009).
- [5] A. E. Stuchbery, G. D. Dracoulis, T. Kibédi, A. P. Byrne, B. Fabricius, A. R. Poletti, G. J. Lane, and A. M. Baxter, *Nucl. Phys. A* **548**, 159 (1992).
- [6] A. P. Byrne, G. J. Lane, G. D. Dracoulis, B. Fabricius, T. Kibédi, A. Stuchbery, A. M. Baxter, and K. J. Schiffer, *Nucl. Phys. A* **567**, 445 (1994).
- [7] A. P. Byrne, R. Müsseler, H. Hübel, M. Murzel, K. Theine, W. Schmitz, K. H. Maier, H. Kluge, H. Grawe, and H. Haas, *Phys. Lett. B* **217**, 38 (1989).
- [8] S. Bayer, A. P. Byrne, G. D. Dracoulis, A. M. Baxter, T. Kibédi, F. G. Kondev, S. M. Mullins, and T. R. McGoram, *Nucl. Phys. A* **650**, 3 (1999).
- [9] A. E. Stuchbery, G. D. Dracoulis, A. P. Byrne, S. J. Poletti, and A. R. Poletti, *Nucl. Phys. A* **482**, 692 (1988).
- [10] S. J. Poletti, G. D. Dracoulis, A. R. Poletti, A. P. Byrne, A. E. Stuchbery, and J. Gerl, *Nucl. Phys. A* **448**, 189 (1986).
- [11] G. D. Dracoulis, C. A. Steed, A. P. Byrne, S. J. Poletti, A. E. Stuchbery, and R. A. Bark, *Nucl. Phys. A* **462**, 576 (1987).
- [12] L. P. Gaffney *et al.*, *Nature (London)* **497**, 199 (2013).
- [13] I. Ahmad and P. A. Butler, *Annu. Rev. Nucl. Part. Sci.* **43**, 71 (1993), and references therein.
- [14] P. A. Butler, *J. Phys. G: Nucl. Part. Phys.* **43**, 073002 (2016).
- [15] S. C. Panchoi, *Pear Shaped Nuclei* (World Scientific, Singapore, 2020).
- [16] P. M. Walker and N. Minkov, *Phys. Lett. B* **694**, 119 (2010).
- [17] M. W. Drigert, J. A. Cizewski, and M. S. Rosenthal, *Phys. Rev. C* **32**, 136 (1985).
- [18] M. Aïche, A. Chevallier, J. Chevallier, S. Hulne, S. Khazrouni, N. Schulz, and J. C. Sens, *J. Phys. G: Nucl. Phys.* **14**, 1191 (1988).
- [19] Pragati, A. Y. Deo, S. K. Tandel, S. S. Bhattacharjee, S. Chakraborty, S. Rai, S. G. Wahid, S. Kumar, S. Muralithar, R. P. Singh, I. Bala, R. Garg, and A. K. Jain, *Phys. Rev. C* **97**, 044309 (2018).
- [20] J. Kurcewicz, W. Czarnacki, M. Karny, M. Kasztelan, M. Kisieliński, A. Korgul, W. Kurcewicz, J. Kurpeta, S. Lewandowski, P. Majorzewicz, H. Penttilä, A. Plochocki, B. Roussière, O. Steczkiewicz, and A. Wojtasiewicz, *Phys. Rev. C* **76**, 054320 (2007).
- [21] R. E. Eppley and E. K. Hyde, Lawrence Radiation Laboratory Report No. UCRL-20426, 1971 (unpublished), p. 27.

- [22] R. K. Sheline, C. F. Liang, P. Paris, and A. Gizon, *Phys. Rev. C* **55**, 1162 (1997).
- [23] A. Krämer-Flecken, T. Morek, R. M. Lieder, W. Gast, G. Hebbinghaus, H. M. Jäger, and W. Urban, *Nucl. Instrum. Methods Phys. Res., Sect. A* **275**, 333 (1989).
- [24] G. Duchêne, F. A. Beck, P. J. Twin, G. de France, D. Kurien, L. Han, C. W. Beausang, M. A. Bentley, P. J. Nolan, and J. Simpson, *Nucl. Instrum. Methods Phys. Res. Sect. A* **432**, 90 (1999).
- [25] J.-M. Régis, G. Pascovici, J. Jolie, and M. Rudigier, *Nucl. Instrum. Methods Phys. Res., Sect. A* **622**, 83 (2010), and references therein.
- [26] R. Brun and F. Rademakers, *Nucl. Instrum. Methods Phys. Res., Sect. A* **389**, 81 (1997).
- [27] Pragati, A. Y. Deo, Khamosh Yadav, Madhu, P. C. Srivastava, S. K. Tandel, S. G. Wahid, G. H. Bhat, Y. Y. Wang, S. Kumar, S. Muralithar, R. P. Singh, Indu Bala, S. S. Bhattacharjee, Ritika Garg, S. Chakraborty, S. Rai, S. Jehangir, J. A. Sheikh, S. Q. Zhang, J. Meng, and A. K. Jain (unpublished).
- [28] K. Yadav, A. Y. Deo, Pragati, S. K. Tandel, S. S. Bhattacharjee, S. Chakraborty, S. Rai, S. G. Wahid, S. Kumar, S. Muralithar, R. P. Singh, I. Bala, R. Garg, and A. K. Jain, in *Proceedings of DAE Symposium on Nuclear Physics*, Vol. 63 (DAE-BRNS, Bhabha Atomic Research Centre, India, 2018), p. 182.
- [29] G. D. Dracoulis, P. M. Walker, and F. G. Kondev, *Rep. Prog. Phys.* **79**, 076301 (2016).
- [30] A. K. Jain, B. Maheshwari, S. Garg, M. Patial, and B. Singh, *Nucl. Data Sheets* **128**, 1 (2015).
- [31] A. P. Byrne, S. Bayer, G. D. Dracoulis, and T. Kibédi, *Phys. Rev. Lett.* **80**, 2077 (1998).
- [32] P. Alexa and R. K. Sheline, *Phys. Rev. C* **56**, 3087 (1997).
- [33] T. P. Sjoreen, U. Garg, D. B. Fossan, J. R. Beene, T. K. Alexander, E. D. Earle, O. Häusser, and A. B. McDonald, *Phys. Rev. C* **20**, 960 (1979).
- [34] M. E. Debray, A. J. Kreiner, M. Davidson, J. Davidson, D. Hojman, D. Santos, V. R. Vanin, N. Schulz, M. Aiche, A. Chevallier, J. Chevallier, and J. C. Sens, *Nucl. Phys. A* **568**, 141 (1994).
- [35] M. E. Debray, J. Davidson, M. Davidson, A. J. Kreiner, D. Hojman, D. Santos, K. Ahn, D. B. Fossan, Y. Liang, R. Ma, E. S. Paul, W. F. Piel, Jr., and N. Xu, *Phys. Rev. C* **41**, R1895 (1990).
- [36] S. Frauendorf, Y. Gu, and J. Sun, *Int. J. Mod. Phys. E* **20**, 465 (2011).
- [37] L. Coraggio, A. Covello, A. Gargano, and N. Itaco, *Phys. Rev. C* **80**, 021305(R) (2009).
- [38] N. Shimizu, T. Mizusaki, Y. Utsuno, and Y. Tsunoda, *Comput. Phys. Commun.* **244**, 372 (2019).
- [39] L. Coraggio, A. Covello, A. Gargano, and N. Itaco, *Phys. Rev. C* **76**, 061303(R) (2007).
- [40] J. Suhonen, *From Nucleons to Nucleus: Concepts of Microscopic Nuclear Theory* (Springer, Berlin, 2006), p. 68.
- [41] O. J. Roberts, C. R. Nita, A. M. Bruce, N. Marginean, D. Bucurescu, D. Deleanu, D. Filipescu, N. M. Florea, I. Gheorghe, D. Ghita, T. Glodariu, R. Lica, R. Marginean, C. Mihai, A. Negret, T. Sava, L. Stroe, R. Suvaila, S. Toma, T. Alharbi, T. Alexander, S. Aydin, B. A. Brown, F. Browne, R. J. Carroll, K. Mulholland, Z. Podolyak, P. H. Regan, J. F. Smith, M. Smolen, and C. M. Townsley, *Phys. Rev. C* **93**, 014309 (2016).
- [42] A. E. Stuchbery, in *XXXVI Brazilian Workshop on Nuclear Physics, 1–5 September 2013, São Sebastião, Brazil*, edited by M. H. Tabacniks, J. R. Brandão de Oliveira, J. M. Barbosa Shorto, and R. Higa, AIP Conf. Proc. No. 1625 (AIP, New York, 2014), p. 52.
- [43] W. Nazarewicz, G. A. Leander, and J. Dudek, *Nucl. Phys. A* **467**, 437 (1987).
- [44] G. Maquart *et al.*, *Phys. Rev. C* **95**, 034304 (2017).
- [45] W. Urban, R. M. Lieder, W. Gast, G. Hebbinghaus, A. Kramer-Flecken, K. P. Blume, and H. Hubel, *Phys. Lett. B* **185**, 331 (1987).
- [46] N. Roy, D. J. Decman, H. Kluge, K. H. Maier, A. Maj, C. Mittag, J. Fernandez-Niello, H. Puchta, and F. Riess, *Nucl. Phys. A* **426**, 379 (1984).
- [47] G. D. Dracoulis, F. Riesz, A. M. Baxter, and A. E. Stuchbery, *J. Phys. G: Nucl. Part. Phys.* **17**, 1795 (1991).
- [48] S.-C. Wu, *Nucl. Data Sheets* **108**, 1057 (2007).
- [49] D. J. Decman, H. Grawe, H. Kluge, K. H. Maier, A. Maj, M. Menningen, N. Ray, and W. Wiegner, *Nucl. Phys. A* **419**, 163 (1984).